Neurobiology of Disease

Dysregulation of Neuronal Ca^{2+} Channel Linked to Heightened Sympathetic Phenotype in Prohypertensive States

Hege E. Larsen,[1,2] Emma N. Bardsley,[1,2] Konstantinos Lefkimmiatis,[2] and David J. Paterson[1,2]
[1]OXION Initiative in Ion Channels and Disease and [2]Burdon Sanderson Cardiac Science Center, Department of Physiology, Anatomy and Genetics, University of Oxford, Oxford OX1 3PT, United Kingdom

Hypertension is associated with impaired nitric oxide (NO)–cyclic nucleotide (CN)-coupled intracellular calcium (Ca^{2+}) homeostasis that enhances cardiac sympathetic neurotransmission. Because neuronal membrane Ca^{2+} currents are reduced by NO-activated S-nitrosylation, we tested whether CNs affect membrane channel conductance directly in neurons isolated from the stellate ganglia of spontaneously hypertensive rats (SHRs) and their normotensive controls. Using voltage-clamp and cAMP–protein kinase A (PKA) FRET sensors, we hypothesized that impaired CN regulation provides a direct link to abnormal signaling of neuronal calcium channels in the SHR and that targeting cGMP can restore the channel phenotype. We found significantly larger whole-cell Ca^{2+} currents from diseased neurons that were largely mediated by the *N*-type Ca^{2+} channel ($Cav_{2.2}$). Elevating cGMP restored the SHR Ca^{2+} current to levels seen in normal neurons that were not affected by cGMP. cGMP also decreased cAMP levels and PKA activity in diseased neurons. In contrast, cAMP–PKA activity was increased in normal neurons, suggesting differential switching in phosphodiesterase (PDE) activity. PDE2A inhibition enhanced the Ca^{2+} current in normal neurons to a conductance similar to that seen in SHR neurons, whereas the inhibitor slightly decreased the current in diseased neurons. Pharmacological evidence supported a switching from cGMP acting via PDE3 in control neurons to PDE2A in SHR neurons in the modulation of the Ca^{2+} current. Our data suggest that a disturbance in the regulation of PDE-coupled CNs linked to *N*-type Ca^{2+} channels is an early hallmark of the prohypertensive phenotype associated with intracellular Ca^{2+} impairment underpinning sympathetic dysautonomia.

Key words: autonomic nervous system; cGMP; dysautonomia; hypertension; *N*-type Ca^{2+} channel; sympathetic

Significance Statement

Here, we identify dysregulation of cyclic-nucleotide (CN)-linked neuronal Ca^{2+} channel activity that could provide the trigger for the enhanced sympathetic neurotransmission observed in the prohypertensive state. Furthermore, we provide evidence that increasing cGMP rescues the channel phenotype and restores ion channel activity to levels seen in normal neurons. We also observed CN cross-talk in sympathetic neurons that may be related to a differential switching in phosphodiesterase activity. The presence of these early molecular changes in asymptomatic, prohypertensive animals could facilitate the identification of novel therapeutic targets with which to modulate intracellular Ca^{2+}. Turning down the gain of sympathetic hyperresponsiveness in cardiovascular disease associated with sympathetic dysautonomia would have significant therapeutic utility.

Introduction

Increased activity of the sympathetic nervous system is a well established contributing factor to the pathophysiology of human hypertension (Esler, 2010; Grassi et al., 2015) and to that observed in the spontaneously hypertensive rat (SHR) (Heaton et al., 2006; Shanks et al., 2013a; Mancia and Grassi, 2014). In par-

Received March 31, 2016; revised May 13, 2016; accepted May 27, 2016.

Author contributions: H.E.L. and D.J.P. designed research; H.E.L. and E.N.B. performed research; K.L. contributed unpublished reagents/analytic tools; H.E.L. and E.N.B. analyzed data; H.E.L. and D.J.P. wrote the paper.

This project was supported by the Wellcome Trust (OXION) and the British Heart Foundation Center of Research Excellence. We thank Professor Manuela Zaccolo and Dr. Dan Li for technical assistance and advice regarding the FRET experiments and Professor Nigel Emptage and Professor Neil Herring for advice concerning the electrophysiological measurements.

The authors declare no competing financial interests.

This article is freely available online through the *J Neurosci* Author Open Choice option.

Correspondence should be addressed to David J. Paterson, Burdon Sanderson Cardiac Science Center, Department of Physiology, Anatomy and Genetics, University of Oxford, Parks Road, OX1 3PT Oxford, UK. E-mail: david.paterson@dpag.ox.ac.uk.

DOI:10.1523/JNEUROSCI.1059-16.2016

ticular, the renal nerves (Lundin et al., 1984) and the postganglionic nerves innervating the heart are sympathetic beds associated with heightened activity. Interestingly, this sympathetic impairment occurs in young, prohypertensive animals (Li et al., 2012; Shanks et al., 2013c), suggesting that it is an early hallmark of the disease itself, although the exact mechanisms that underpin the phenotype remain poorly understood. When postganglionic sympathetic stellate neurons (PGSNs) that predominantly innervate the heart from age-matched prohypertensive SHRs are compared with PGSNs from normotensive rats (WKY), the SHR neurons have increased intracellular calcium transients ($[Ca^{2+}]_i$) (Li et al., 2012) and enhanced neurotransmission (Zugck et al., 2003; Li et al., 2007; Shanks and Herring, 2013; Shanks et al., 2013c). This translates into increased postsynaptic excitability of the sinoatrial node due to a greater conductance of ICa_L^{2+} and an increase in heart rate (Heaton et al., 2006). The observed differences in $[Ca^{2+}]_i$ may be partially explained by altered mitochondrial Ca^{2+} handling (Li et al., 2012), but it is unclear whether there are additional changes at the membrane level that contribute to the greater calcium transients.

Recently, Tu et al. (2014) demonstrated enhanced activity of the *N*-type voltage-gated Ca^{2+} ($Cav_{2.2}$) channel in the PGSNs of a rat model of heart failure. Another study found that inhibition of this channel restores cardiac autonomic imbalance and prevents lethal arrhythmias in a mouse model of heart failure (Yamada et al., 2014). Similarly, we also observed increased whole-cell neuronal Ca^{2+} currents in the prohypertensive SHR (Lu et al., 2015), suggesting that channel dysregulation is an early molecular event that may be highly conserved over several developmental stages from the prediseased phenotype to advanced heart failure (Li and Paterson, 2016). What links ion channel dysregulation to sympathetic hyperresponsiveness? One suggestion is that early metabolic-oxidative stress could be coupled to abnormal cyclic nucleotide (CN) regulation (Krukoff, 1998; Danson and Paterson, 2005; Danson et al., 2005). Voltage-gated Ca^{2+} channels are strongly regulated by CN-coupled protein kinases (Catterall, 2000; Simms and Zamponi, 2014) that are dysfunctional in hypertension (Paterson, 2001; Heaton et al., 2007; Li et al., 2007; Wang et al., 2007; Li et al., 2013). Specifically, PGSNs have reduced neuronal nitric oxide synthase (nNOS) activity, low level expression of soluble guanylyl cyclase (sGC) (Li et al., 2013) and high phosphodiesterase 2A (PDE2A) activity (Li et al., 2015), leading to reduced levels of cGMP (Li et al., 2007, 2013). Together, this cascade of events could provide a link to ion channel dysregulation. However, emerging evidence suggests that the inhibitory action of NO donors on $Cav_{2.2}$ in HEK 293 cells is via cGMP-independent pathways coupled to S-nitrosylation of the *N*-type channel (Jin et al., 2011; Zhou et al., 2015).

Here, we tested the hypothesis that impaired CN regulation provides a direct link to abnormal signaling of neuronal calcium channels in prohypertensive rats and that targeting cGMP can restore the normal channel phenotype in the diseased PGSN.

Materials and Methods

Animals. Four-week-old male prohypertensive SHRs and normotensive WKY and Wistar (hereafter referred to as control) rats were obtained from Harlan Laboratories and Charles River Laboratories. The SHRs begin to show development of clinical symptoms of hypertension at 6 weeks of age (Dickhout and Lee, 1998). The rats were housed in standard plastic cages and artificial lighting was fixed to a natural 12 h light/dark cycle. Food and water were available *ad libitum*. All experiments were performed in accordance with the UK Home Office Animals Scientific Procedures Act of 1986 (PPL 30/2360 and 30/3131, David J. Paterson).

Reagents. All drugs and reagents were sourced from Sigma-Aldrich unless stated otherwise.

Adenovirus generation. The complete open reading frame of the cAMP-sensitive FRET-based sensor H187 was obtained from pcDNA3 using double digestion with the restriction enzymes EcoRI and HindIII and introduced in the pDual vector. Generation and amplification of the viral particles were outsourced to Vector Biolabs.

Cell isolation. The sympathetic stellate neurons that predominately innervate the heart were isolated as described previously (Shanks et al., 2013b). Briefly, the stellate neurons from 4-week-old prohypertensive SHR and normotensive control rats were dissected out and digested with collagenase (1 mg/ml) and trypsin (2 mg/ml) to create a single-cell suspension. The PGSNs were then grown on 6 mm poly-D-lysine/laminin-coated coverslips (37°C 5% CO_2) for 3 h before electrophysiological recordings were made. For measurements of intracellular cAMP and protein kinase A (PKA), PGSNs were transfected with relevant adenoviral particle-forming units (H187:1.4×10^7, AKAR4: 4×10^9) for 24 h. The cells were incubated for 24–48 h before FRET imaging.

Immunofluoresence. Cells were fixed with 4% formaldehyde for 10 min before blocking and permeabilization using a solution containing 10% goat serum, 0.3% bovine serum albumin, and 0.1% Triton X-100 in PBS for 1 h at room temperature. After washes with PBS, primary antibodies against tyrosine hydroxylase (TH, 1:250, T1299; Abcam) and $Cav_{2.2}$ (1:250, ACC-002; Alomone Laboratories) were incubated overnight at 4°C. Appropriate secondary antibodies (Alexa Fluor 1:1000) were added for 2 h before the coverslips were mounted using mounting medium containing DAPI (Vectashield; Vector Laboratories). Cells were imaged on a confocal microscope (Live Cell; Olympus) within 1 week of mounting.

Whole-cell voltage clamp of acutely isolated neurons. Voltage-clamp experiments were conducted using the Axopatch 200B amplifier and Clampex software. The neurons were held at −90 mV before a set of 50 ms voltage steps from −50 to +50 were applied with 10 mV, 5 s intervals. The bath was grounded using an Ag/AgCl silver pellet wire connected to the bath via a 3 M agar salt bridge. Cells were perfused with tyrode or Ca^{2+}-isolating solution using a custom-built perfusion system into a heated microscope stage chamber maintained at 37°C. Access to the cell was obtained in normal tyrode solution containing the following (in mM): 135 NaCl, 4.5 KCl, 11 glucose, 20 HEPES, $1MgCl_2$, 2 $CaCl_2$, pH 7.4. Then, the solution was changed to the Ca^{2+}-isolating solution containing no Na^+ and K^+ channel blockers (TEA and Cs^+) with Ba^{2+} as the charge carrier to isolate the Ca^{2+} currents containing the following (in mM): 135 TEACl, 10 HEPES, 4.5 KCl, 1 $MgCl_2$, 4 glucose, 1 $NaHCO_3$, 2 Ba^{2+}, pH 7.40, either in the presence or absence of drugs (1 μM ω-conotoxin GVIA or 100 μM 8 bromoguanosine-cGMP, 8b-cGMP). Ba^{2+} was used as the charge carrier to avoid Ca^{2+}-dependent current inactivation (Imredy and Yue, 1994). The internal solution contained the following (in mM): 140 CsCl, 10 HEPES, 0.1 $CaCl_2$, 1 $MgCl_2$, 4 MgATP, 1 EGTA, pH 7.30. All solutions had osmolarities of 300 mOsm/L. A 75–90% series resistance compensation was applied to all cells. Peripheral neurons portray significant axonal branching, making an effective voltage clamp difficult to achieve (Bar-Yehuda and Korngreen, 2008). To minimize these space-clamp errors, the cells were held at −90 mV, low concentrations of the charge carrier was used, cells were patched acutely, and large bore, blunt electrodes (1.5–2 MΩ) were used in addition to strict exclusion criteria. Only cells that had a series resistance of <10 MΩ throughout the recording, a holding potential of >−300 pA, and cells in which no visible contusion of the currents were visible were included in this study. Due to significant run-down of the currents in both animal models, which was found to be neither time nor activity dependent, unpaired experiments were performed to unmask differences between cells.

FRET measurements of cytosolic cAMP and PKA activity. For intracellular measurements of cAMP and PKA activity, cells were infected 0–24 h after culture with the FRET-based cAMP sensors Epac-H30 (Ponsioen et al., 2004), Epac-H187 (Klarenbeek et al., 2015) or the PKA sensor AKAR4 (Depry et al., 2011; Lefkimmiatis et al., 2013) for 24 h. FRET sensor-expressing neurons were imaged 3–4 d after isolation on an inverted Nikon microscope. This was connected to an OptoLED fluores-

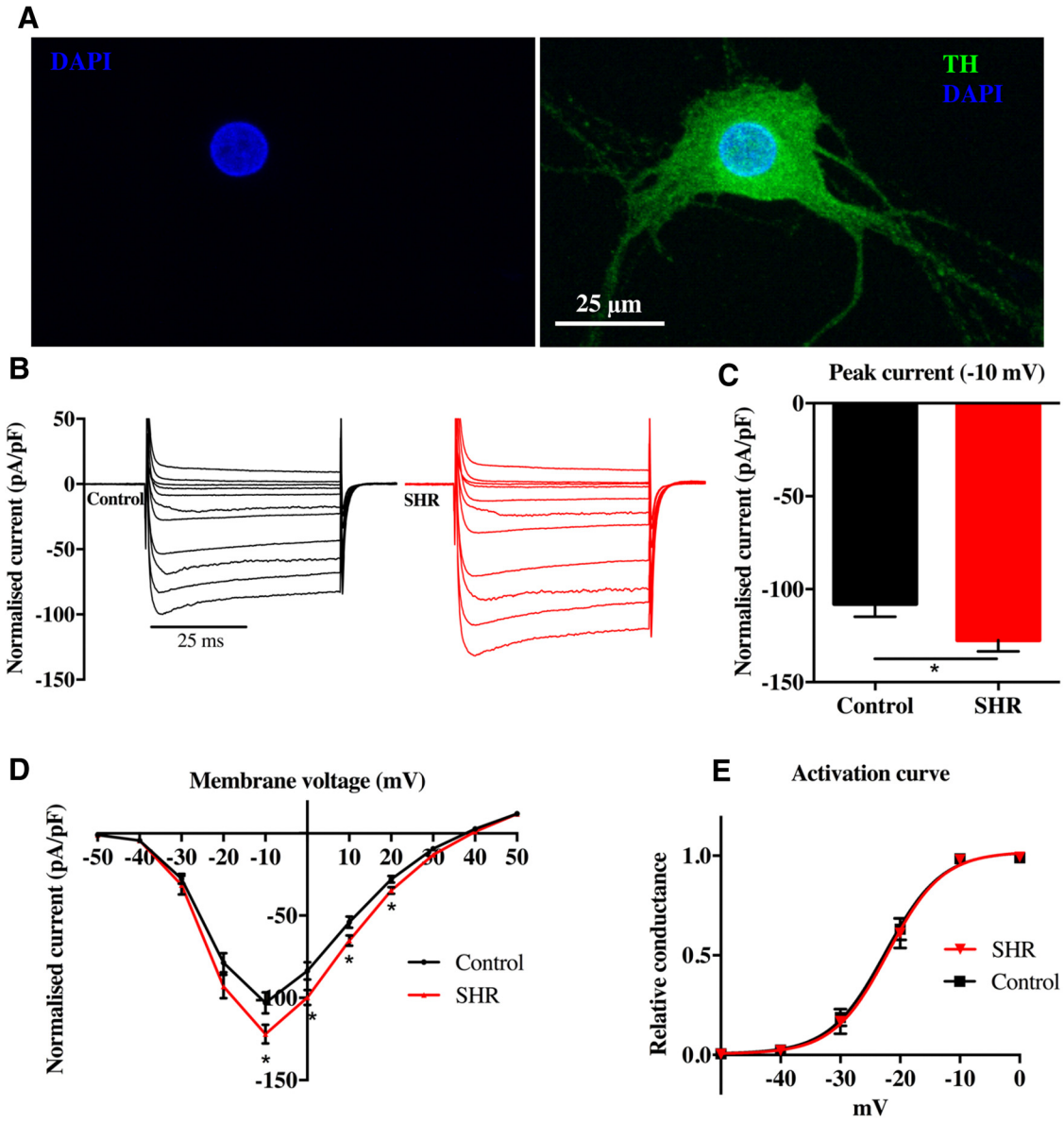

Figure 1. The whole-cell Ca^{2+} current is larger in the prohypertensive SHR. Whole-cell voltage clamp was performed on the cardiac sympathetic stellate ganglion innervating the heart to investigate the whole-cell Ca^{2+} properties of 4-week-old prohypertensive SHR and normotensive control rats; 50 ms, 10 mV voltage steps from −50 to +50 were applied to the cell before the resulting current was measured. Immunofluoresence showed TH positivity, confirming sympathetic phenotype of the neurons (***A***). ***B***, Representative voltage-clamp traces of control and SHR neurons showing significantly larger currents in the SHR neurons. ***C***, Peak current (−10 mV) was −127.5 ± 5.94 pA/pF ($n = 10$) in the SHR and −108.0 ± 6.80 pA/pF ($n = 10$, $p < 0.045$) in the control. ***D***, Current–voltage relationship showing significantly larger currents in the SHR compared with the control at multiple voltages. ***E***, There were no changes in the voltage dependency of the channel, as shown by the activation curve, suggesting that the biophysical properties of the channels are unaffected. Data are represented as the mean ± SEM.

cence imaging system (Cairn Research) equipped with a 40× oil-immersion objective, a CoolSnap HQ2 digital CCD camera (Photometics), and a beam-splitter (DV2; Photometrics), which included the emission filters for CFP and YFP acquisition (dichroic mirror 505DCXR). The cells were excited at 430 nm for 100 ms every 15 s. CFP and YFP emissions were measured and the ratio between 480/535 nm fluorescent emission intensities were automatically calculated using Optofluor software. Background fluorescence was subtracted from emission intensities and intensity ratios were plotted against time. Mean FRET responses were expressed as the percentage change from baseline ($\Delta R/R_0$ where $\Delta_R = R - R_0$. R_0 is the ratio of intensity over a 30 s period in the absence of drugs and R is the mean ratio over 30 s in the presence of the respective drug treatment).

During FRET experiments, cells were perfused continuously with Tyrode's solution and flow rate was controlled at 2–3 ml/min. Pharmacological agents were diluted in Tyrode's solution and perfused at the following concentrations: forskolin, 0–25 μM; 3-isobutyl-1-methylxanthine (IBMX), 1–100 μM; the cGMP analog 8b-cGMP, 100 μM; the PDE3 inhibitors cilostamide, 10 μM, or milrinone, 10 μM; and the PDE2 inhibitor BAY-60-7550, 1 μM (Cayman Chemicals). For comparisons between cells, the average percentage FRET change over a 30 s period was calculated once equilibrium was reached. In all experiments, the maximal FRET change of each cell was recorded by exposing the cells to saturating concentrations of an adenylyl cyclase (AC) activator and a PDE inhibitor (25 μM forskolin and 100 μM IBMX, respectively) to ensure that the cells responded similarly to the sensor. The H30 cAMP sensor responded differently in the SHR and control cells, so these data were normalized to the IBMX/forskolin maximum FRET response to allow for comparisons between the control and SHR neurons.

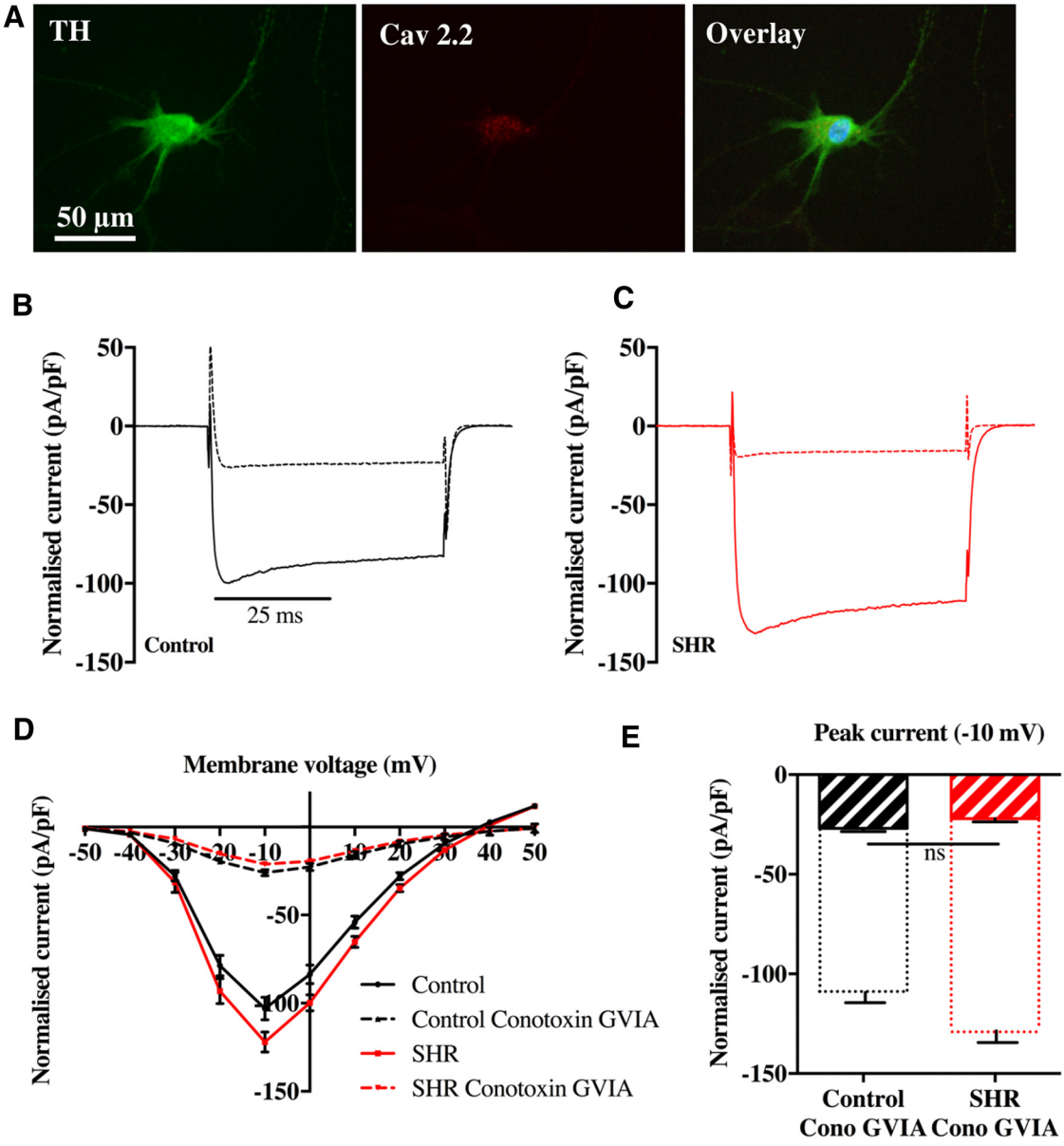

Figure 2. 1 μM conotoxin GVIA blocks 75% and 83% of the current, suggesting that the *N*-type Ca^{2+} channel is the major contributor to ionic conductance. ***A***, Immunofluorescence showing TH positivity and cell surface expression of the *N*-type Ca^{2+} channel. The nuclear stain DAPI is included on the overlay image. Representative peak (−10 mV) voltage-clamp traces of control (***B***) and SHR (***C***) in normal conditions (solid lines) and after treatment with conotoxin GVIA (dashed lines). ***D***, Current–voltage relationship showing uniform reduction in both the SHR and control neurons at multiple voltages. The peak current remains at −10 mV and is not significantly different between the control and SHR. ***E***, Bar chart of the peak currents (−10 mV) showing a 75% (control) and 83% (SHR) reduction of the *N*-type Ca^{2+} current down to levels that were not significantly different between the strains (−26.88 ± 1.7 pA/pF, $n = 6$ and −22.04 ± 1.60 pA/pF, $p = 0.07$ $n = 5$). Dashed lines represent the mean of the control (black) and SHR (red) control data. Data are represented as the mean ± SEM.

Protocols. Specifically, we looked at the cells' ability to generate cAMP and resulting PKA activity by administering the AC activator forskolin. Further, we assessed the cells ability to hydrolyze cAMP by pharmacologically inhibiting the predominant PDE subtypes (PDEs 1–7, 10–11) with the nonspecific PDE inhibitor IBMX. To test the involvement of the CNs in the regulation of the *N*-type channel, 8b-cGMP was perfused before the voltage-clamp experiment was repeated. In addition, to investigate whether the cGMP dysfunction seen in the prohypertensive state interferes with the cAMP pathway (through cross-talk via PDEs), we administered 8b-cGMP to the control and SHR neurons and monitored the resulting cAMP levels and PKA activity. Finally, to test the relative involvement of PDE2A and PDE3 in the cells, the cells were incubated with selective PDE2 (1 60–7550) and PDE3 inhibitors (cilostamide or milrione) while the cAMP levels were monitored.

Statistical analysis. All data were analyzed using GraphPad Prism software. When the data passed normality tests, unpaired two-tailed *t* tests were used; when they did not, nonparametric tests were used with the specific test reported in the figure legend. All data are expressed as the mean ± SEM. Statistical significance was accepted at $p < 0.05$.

Results

Neuronal Ca^{2+} currents of the prohypertensive SHR are larger than that of the normotensive control

Immunofluorescence analysis of the cardiac stellate neurons confirmed their sympathetic phenotype by their TH positivity (Fig. 1*A*). The whole-cell voltage-gated Ca^{2+} currents of the prohypertensive SHR (−127.5 ± 5.94 pA/pF, $n = 10$) were significantly larger than that of the normotensive control animals (−108.0 ±

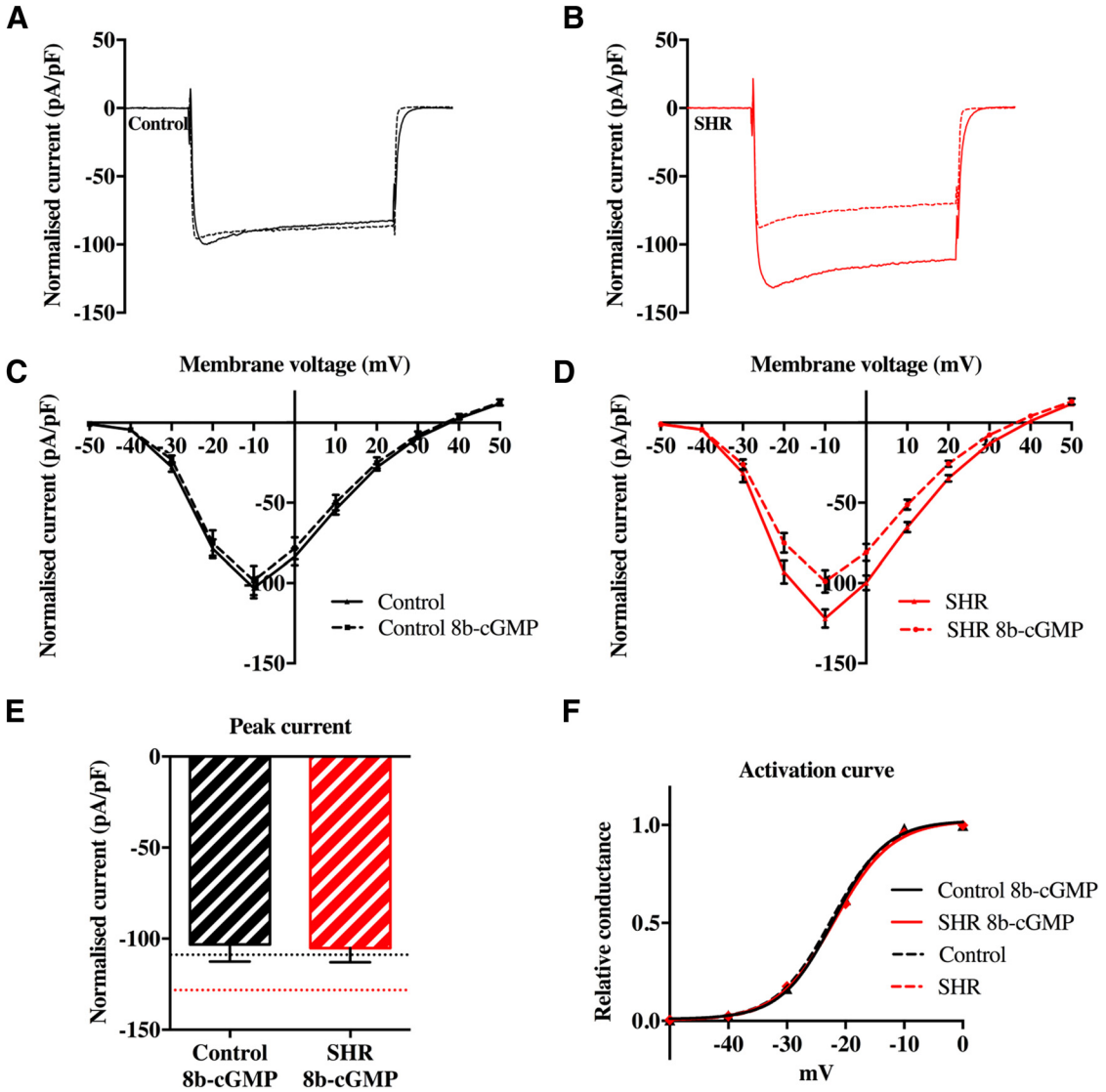

Figure 3. Restoring the cGMP levels rescues the channel phenotype seen in the SHR. Representative peak voltage– clamp traces at −10 mV of control (***A***) and SHR (***B***) neurons showing a decrease in the SHR current after application of 100 μM of a membrane-permeable cGMP analog 8b-cGMP. Current–voltage relationship of control (***C***) and SHR (***D***) neurons shows a normalization of the SHR current down to control levels at all voltages. The peak current remains at −10 mV and is not significantly different from the controls. The drug does not significantly alter the control currents. ***E***, Bar chart of the peak currents (−10 mV) showing a significant reduction and normalization of the SHR current (−127.5 ± 5.94 pA/pF, $n = 10$ to −105.2 ± 7.79 pA/pF, $n = 7$, $p = 0.035$) down to control levels (−108.0 ± 6.80 pA/pF, $n = 10$, $p = 0.79$). Dashed lines represent the mean of the control (black) and SHR (red) control data. ***F***, Activation plot showing no significant difference between the SHR and control or the drug groups, suggesting that the biophysical properties of the channels are unchanged. Data are represented as the mean ± SEM.

6.80 pA/pF, $n = 10$, $p < 0.045$, unpaired t test) at multiple voltages (Fig. 1*B–D*). No significant change in the activation curve was observed (Fig. 1*E*), suggesting that the biophysical properties of the channels were unchanged. No significant difference was observed in cell size (as measured by the cell capacitance in picofarads) or resting membrane potential between the control or SHR neurons (−46.75 ± 0.95 vs −45.40 ± 0.87 mV and 21.36 ± 1.03 vs 21.32 ± 1.17 pF, $n = 32$ and 30, unpaired t test).

Increased whole-cell Ca^{2+} currents are attributed to changes in $Cav_{2.2}$

Immunofluorescence analysis confirmed the expression of the *N*-type Ca^{2+} channels on the membrane of the TH-positive cells (Fig. 2*A*). We tested their functional relevance by perfusing the cells with 1 μM ω-conotoxin GVIA and observed a reduction in the whole-cell currents by 75% and 83%, respectively, down to similar levels in both normotensive and hypertensive phenotypes (control −26.88 ± 1.70, $n = 6$; SHR −22.04 ± 1.60 pA/pF, $n = 5$, $p = 0.072$), suggesting that $Ca_{v2.2}$ is the Ca^{2+} channel predominantly carrying the Ca^{2+} current in PGSNs (Fig. 2*B–E*).

Increasing the intracellular cGMP concentrations significantly lowers Ca^{2+} currents and reverses the channel phenotype

To test the involvement of the CNs in the regulation of the *N*-type channel, the cell-permeant 8b-cGMP was perfused before the voltage-clamp experiment was repeated. Elevating intracellular cGMP did not alter the Ca^{2+} currents in the normotensive control animals, but reduced the SHR currents (−127.5 ± 5.94 pA/pF, $n = 10$ to −105.2 ± 7.79 pA/pF, $n = 7$, $p = 0.035$) down to levels seen in the control animals (−108.0 ± 6.80 pA/pF, $n = 10$, $p = 0.79$; Fig. 3*A–E*). No changes were observed in the activation curve (Fig. 3*F*).

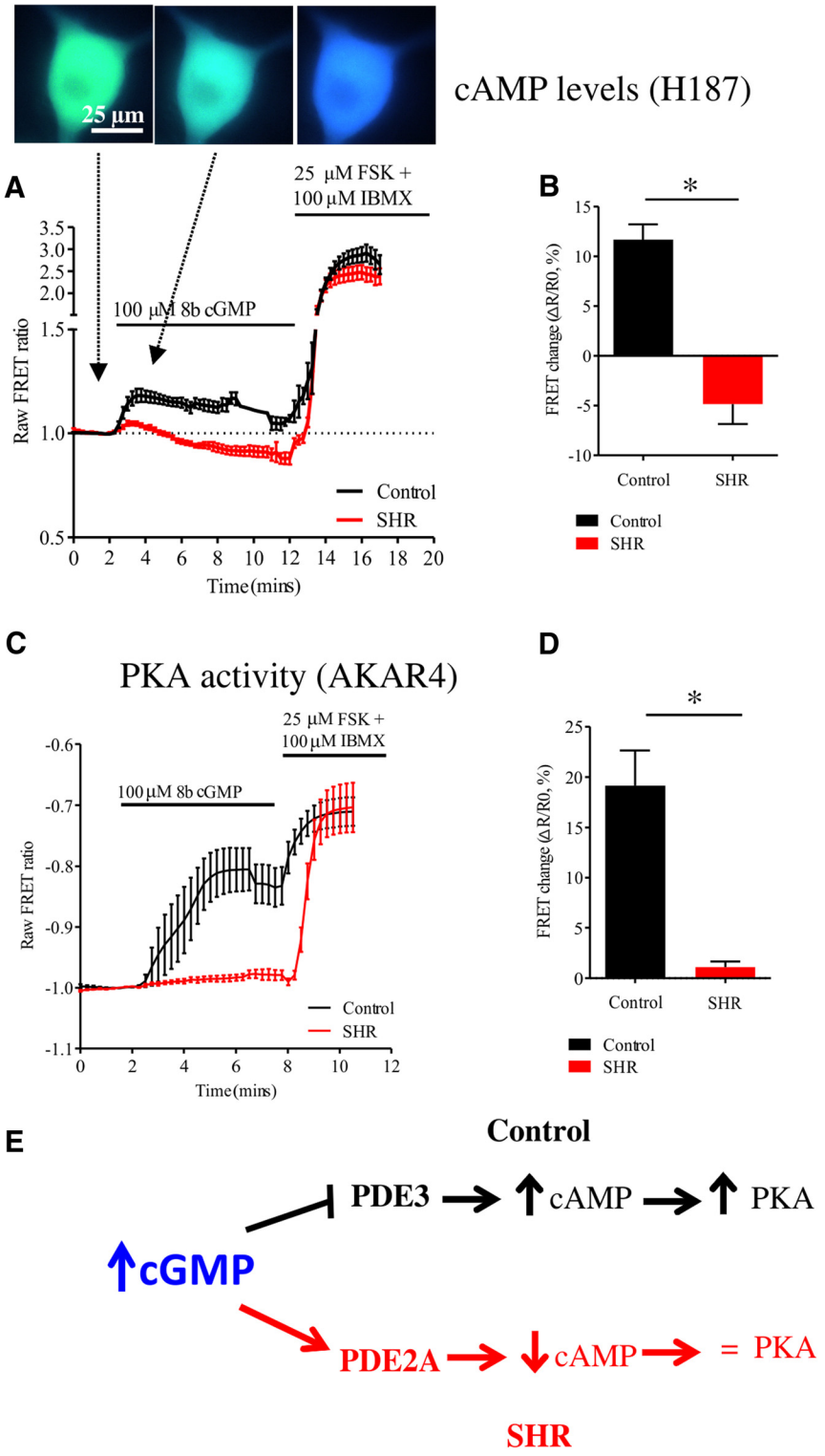

Figure 4. Differential cGMP– cAMP cross-talk in the SHR. In the control cells, 8b-cGMP application results in an increase in cAMP levels, but a reduction in the SHR neurons (11.68 ± 1.54% vs −4.82 ± 2.02%, $p < 0.0001$, unpaired t test, $n = 14–16$; ***A***, ***B***). As a result, the PKA activity in the control neurons was found to be significantly higher than that of the SHR (19.15 ± 3.51% vs 1.09 ± 0.57%, $p < 0.0001$, Mann–Whitney test, $n = 6–8$; ***C***, ***D***). These results point toward PDE2A dominance in the SHR, but a greater regulation by a cGMP inhibited PDE in the control cells (***E***).

Differential cGMP-cAMP cross-talk in the SHR

To investigate whether the cGMP dysfunction seen in the prohypertensive state was interfering with the cAMP pathway (through cross-talk via PDEs), we administered 8b-cGMP to the neurons and monitored cAMP levels. We then established the functional relevance of this by assessing PKA activity. Application of 8b-cGMP led to a decrease in cAMP levels (−4.82 ± 2.02%, $n = 14$), with no change in PKA activity (1.09 ± 0.57%, $n = 8$) in the SHR neurons (Fig. 4*A*,*B*). In contrast, when normotensive neurons were treated with 8b-cGMP, we observed a significant increase in both cAMP levels (11.68 ± 1.54% $n = 16$) and PKA activity (19.15 ± 3.51%, $n = 6$; Fig. 4*C*,*D*). This finding suggests a differential involvement of PDE isoforms in response to cGMP signaling in the normotensive versus prohypertensive PGSNs.

Differential response of the SHR and control neurons to PDE2A blockade

PDE2A has been shown recently to play a major role in the control of neurotransmission in sympathetic neurons. To assess whether PDE2A plays a role in regulating Ca^{2+} channels, we bath applied the specific PDE2A inhibitor BAY 60–7550 and repeated the voltage-clamp experiments. The application of 1 µM BAY 60–7550 significantly increased the channel currents (−108.0 ± 6.803 pA/pF, $n = 9$ to −138.7 ± 9.610 pA/pF, $n = 10$, $p = 0.0169$) in the normotensive neurons. Interestingly, the SHR neurons responded to the same treatment with a slight, nonsignificant decrease of currents (−127.5 ± 5.937 pA/pF, $n = 10$ to −118.0 ± 6.673 pA/pF, $n = 9$). After PDE2A inhibition, the control currents were trending toward being larger than the SHR, but this was not quite significant (138.7 ± 9.610 pA/pF to −118.0 ± 6.673 pA/pF, $p = 0.052$; Fig. 5*A–C*).

Sympathetic stellate neurons of the SHR and control rats functionally express both PDE2A and PDE3

To test the relative involvement of PDE2A and PDE3 in the cells, the cells were incubated with selective PDE2A (1 µM BAY 60–7550) and PDE3 inhibitors (10 µM cilostamide or milrinone) while the cAMP levels were monitored. Pharmacological inhibition of PDE2A (Fig. 6*A*) led to significant increases in cAMP in both the control and SHR neurons that was not significantly different (19.69 ± 5.16%, $n = 10$ vs 36.55 ± 21.47%, $n = 8$, $p = 0.94$). The cAMP responses to two separate, clinically tested PDE3 inhibitors led to similar increases in cAMP generation (Fig. 6*B*) that was not significantly different between the SHR and control (milrinone: 22.98 ± 6.81%, $n = 10$ vs 31.14 ± 6.25% $n = 16$, $p = 0.41$; cilostamide: 28.15 ± 15.45%, $n = 5$ vs 33.23 ± 8.18% $n = 8$, $p = 0.58$, Mann–Whitney test).

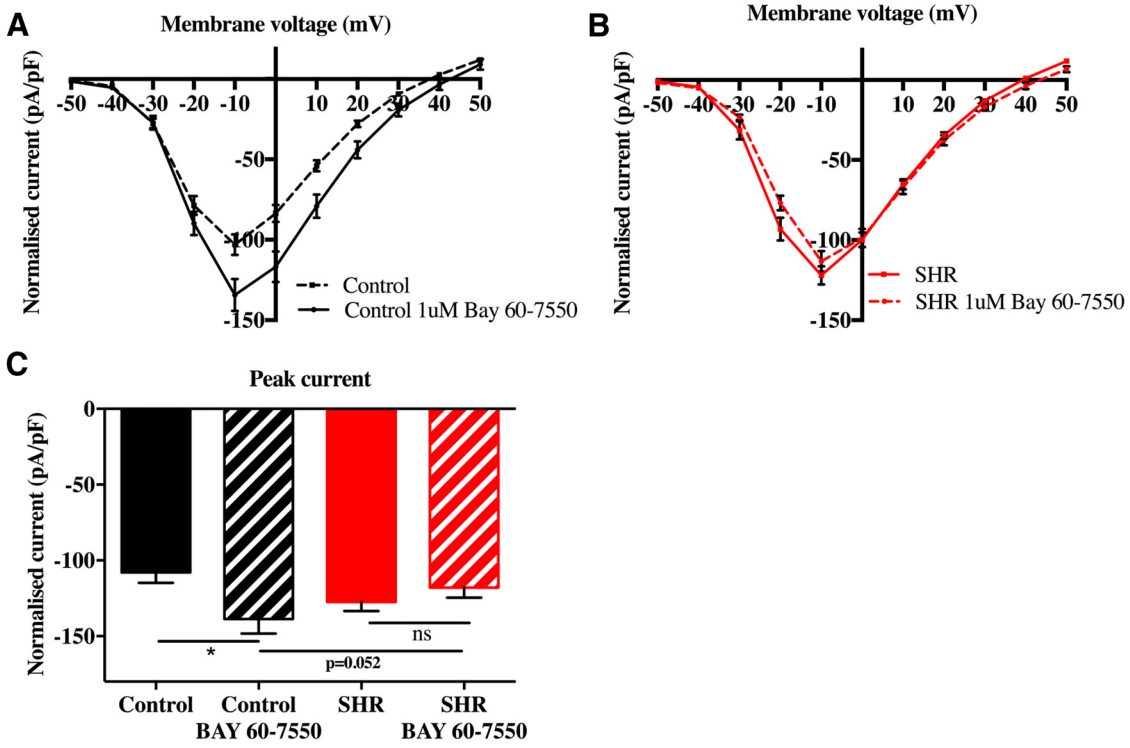

Figure 5. PDE2A blockade suggests differential involvement of PDEs in the control and SHR neurons. Current–voltage relationships of the control (***A***) and SHR (***B***) neurons after the application of 1 μM BAY 60 –7550, a PDE2A-selective inhibitor. BAY 60 –7550 significantly increased the peak control channel currents (-108.0 ± 6.803 pA/pF to -138.7 ± 9.610 pA/pF, $n = 9$ –10, $p = 0.0169$), but showed a slight, nonsignificant decrease on the SHR currents (-127.5 ± 5.937 pA/pF to -118.0 ± 6.673 pA/pF, $p = 0.052$ $n = 10$ and 9). After PDE2A inhibition, the control currents were trending toward being larger than the SHR, but this was not quite significant (138.7 $\pm$ 9.610 pA/pF to -118.0 ± 6.673 pA/pF, $p = 0.052$; ***C***).

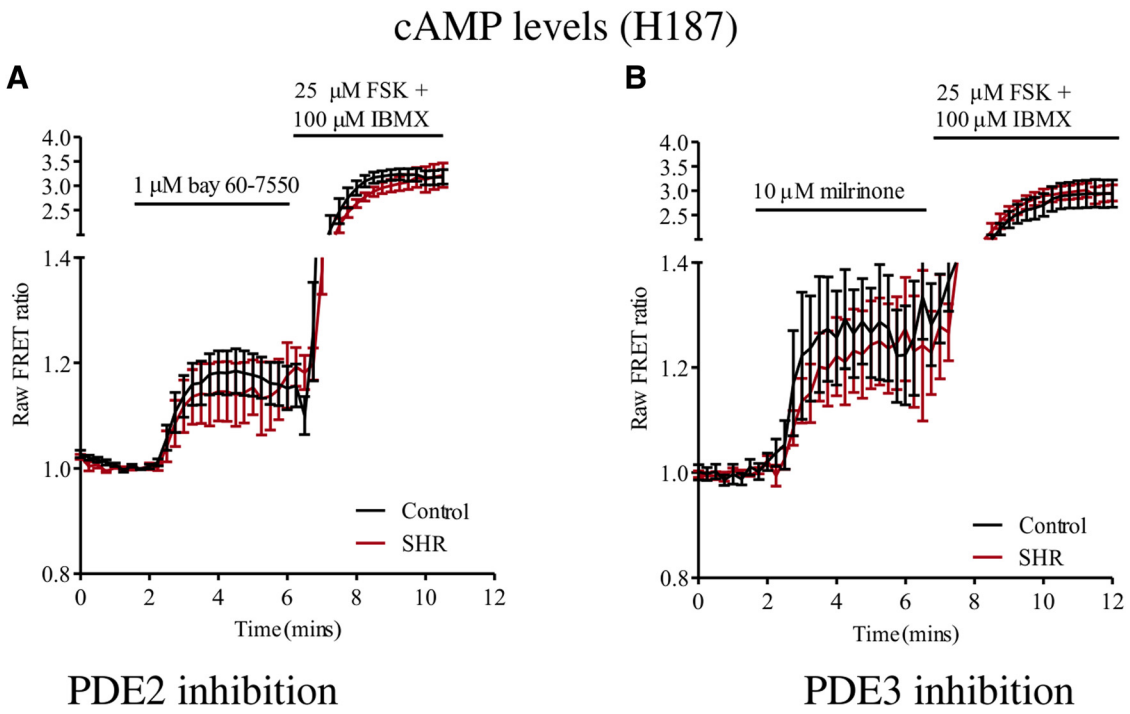

Figure 6. Evidence for the functional expression of PDE2 and PDE3 in the sympathetic neurons of the SHR and WKY. To assess the functional expression of PDE2 and PDE3, FRET imaging of cAMP levels (H187) in response to well characterized PDE-selective blockers was performed. Pharmacological inhibition of PDE2A (1 μM Bay 60 –7550; ***A***) and PDE3 (10 μM milrinone; ***B***) increased the cAMP levels in both the control and SHR neurons. This was found to be nonsignificant between the two strains ($n = 8$ –16; PDE2: 19.69 $\pm$ 5.16%, $n = 10$ vs 36.55 $\pm$ 21.47%, $n = 8$, $p = 0.94$. PDE3: milrinone; 22.98 $\pm$ 6.81%, $n = 10$ vs 31.14 $\pm$ 6.25% $n = 16$, $p = 0.41$. cilostamide; 28.15 $\pm$ 15.45%, $n = 5$ vs 33.23 $\pm$ 8.18% $n = 8$, $p = 0.58$, Mann–Whitney test). The presence of PDE2A in sympathetic stellate neurons is known, but this provides the first evidence for the functional expression of PDE3 in these cells.

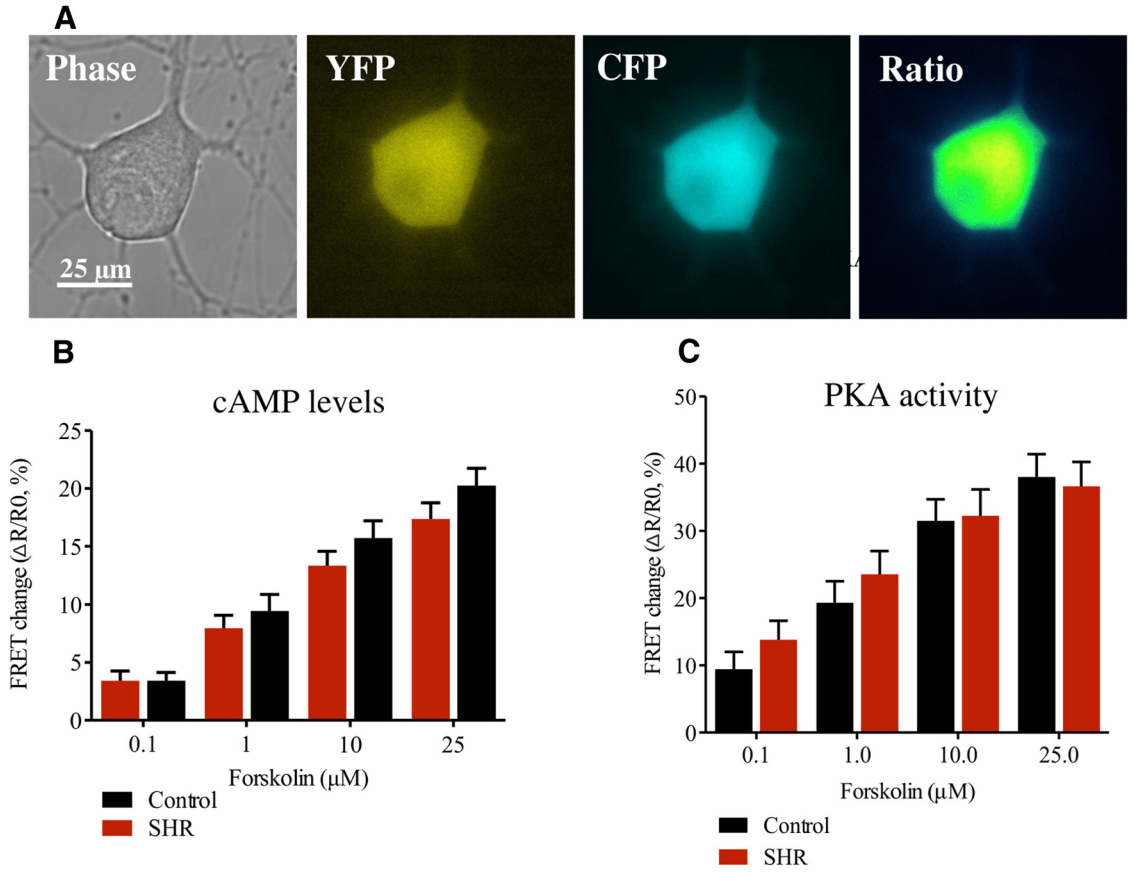

Figure 7. cAMP–PKA signaling pathway is functional in SHR neurons. To investigate the ability of the cells to generate cAMP and PKA, activity was compared between the SHRs and controls using FRET imaging. Cells were infected with the H30 Epac and AKAR sensors and the changes in fluorescence emission intensity of CFP and YFP was monitored (***A***). No significant differences were found in forskolin-induced cAMP generation (***B***) or PKA activity (***C***) in the sympathetic neurons from the prohypertensive SHR or controls. Comparisons were made using the Mann–Whitney test.

cAMP–PKA signaling pathway remains unchanged in prohypertensive animals

To determine the cells' ability to generate cAMP and activate PKA, we administered the AC activator forskolin and measured the FRET responses of the two sensors. FRET experiments in which the PGSNs were challenged with increasing doses of forskolin (0.1–25 μM) revealed no significant difference between the generation of cytosolic cAMP (n = 15–18/21–28), and PKA activity (n = 20–23/16–17) between 4-week normotensive control and pro-SHR, respectively (Fig. 7*A*,*B*). This indicates that the cAMP–PKA signaling pathway remains intact in the prohypertensive animals.

Discussion

The novel findings in this study are as follows. The enhanced whole-cell Ca^{2+} current from the prohypertensive SHR PGSNs are predominately mediated by activation of the *N*-type Ca^{2+} channel. Elevating cGMP restored the SHR Ca^{2+} current to levels seen in normal neurons. Control neurons were unaffected by raised cGMP. Elevated cGMP also decreased cAMP levels and PKA activity in diseased neurons. In contrast, cAMP–PKA activity was increased in normal neurons, suggesting differential switching in PDE activity. PDE2A inhibition enhanced the Ca^{2+} current in normal neurons to a similar conductance to that seen in SHR neurons, whereas the inhibitor slightly decreased the current in diseased neurons. Global cAMP–PKA levels were not different between neurons when activated by an adenylyl cyclase activator. However, pharmacological evidence suggests a switching from cGMP acting via PDE3 in the control neurons to PDE2A in the SHR neurons in the modulation of the *N*-type Ca^{2+} current.

Channel dysfunction in cardiovascular diseases

The importance of the *N*-type Ca^{2+} channel function in relation to the release of noradrenaline (NA) in the sympathetic nervous system has long been known (Molderings et al., 2000; Uhrenholt and Nedergaard, 2005), but its relevance to hypertension came from the observation that *N*-type channel blockade causes hypotension (Pruneau and Bélichard, 1992). Moreover, the $Cav_{2.2}$ mutant mouse has significant problems with blood pressure control that is linked to reduced baroreflex control of heart rate (Ino et al., 2001; Mori et al., 2002). Recently, it was shown that stellate neurons from rats with from heart failure have markedly increased *N*-type channel currents (Tu et al., 2014). Interestingly, the increased current was not correlated with channel expression, suggesting a role for posttranslational regulation of channel activity. Although the *N*-type channel is the major contributor of Ca^{2+} entry coupled to sympathetic transmission (Uhrenholt and Nedergaard, 2003), it is possible that other Ca^{2+} channels are also involved and could account for the residual response that we observed after ω-conotoxin GVIA treatment. Although ω-conotoxin GVIA has high affinity for the *N*-type channel (Olivera et al., 1987), in rat sympathetic neurons, this drug has also been shown to block L-type currents (McCleskey et al., 1986). It is therefore possible that the effect that we observed could be attributed partially to overactivity of this channel in the SHR (Heaton

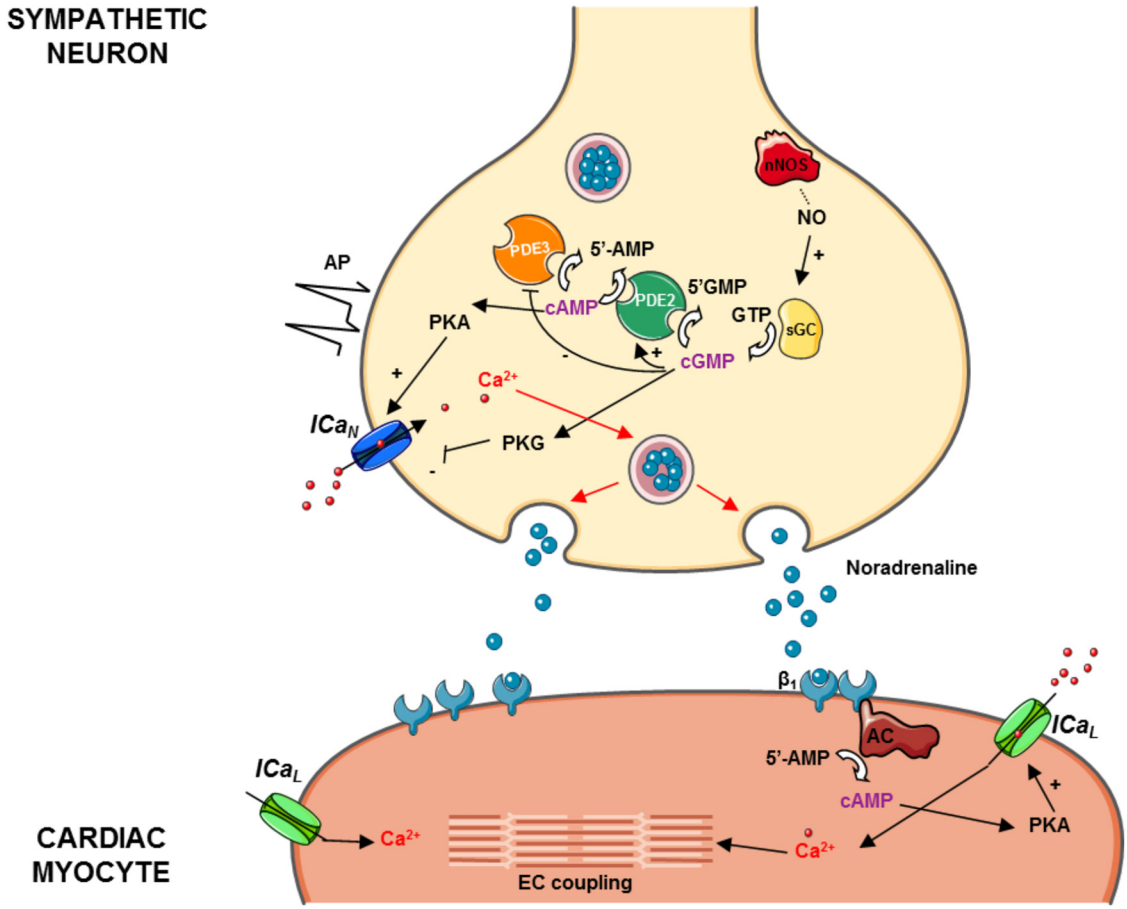

Figure 8. Sympathetic neurotransmission. The arrival of an action potential in the synaptic nerve terminal leads to Ca^{2+} entry via voltage-gated Ca^{2+} channels. This triggers exocytosis of noradrenaline into the synaptic clefts, which acts on the β_1 adrenoreceptor, altering myocyte behavior. In hypertension, nNOS expression and the β_1 subunit of sGC expression is down, resulting in lower levels of cGMP, which, coupled with enhanced PDE2A activity, results in increased neurotransmission. Pharmacological elevation of cGMP reverses the channel phenotype, but also leads to changes in cAMP levels and PKA activity as a result of interactions with PDEs. The differential responses of the control and SHR neurons to cGMP elevation suggests that cAMP levels are controlled by both PDE2A and PDE3 subtypes in the control neurons, but that the prohypertensive phenotype is associated with PDE2A dominance.

et al., 2006) because its inhibition on the mesenteric artery significantly reduces NA release in response to neuronal stimulation (Tsuda et al., 2001). Another possibility is that alterations in cell excitability could be linked to *N*-type Ca^{2+} channel activity. Therefore, we cannot rule out that such changes in threshold or action potential frequency might also be linked with the *N*-type Ca^{2+} channel phenotype. This could conceivably contribute to the overall modulation of channel excitability and enhanced neurotransmission.

CN regulation of Ca^{2+} channels

Ca^{2+} channels are regulated by CNs via PKA- and protein kinase G (PKG)-dependent phosphorylation. cAMP and cGMP act via PKA and PKG to cause activation and inhibition of the channel current, respectively (Bannister et al., 2005; Catterall, 2011; Zamponi et al., 2015). This occurs either via direct phosphorylation of the channels (Tohse and Sperelakis, 1991; Jiang et al., 2000) or through cross-play between the two CN pathways via PDEs (Conti and Beavo, 2007; Zaccolo and Movsesian, 2007; Stangherlin et al., 2011; Stangherlin and Zaccolo, 2012a). CNs also act to terminate their own signals by activating protein phosphatases that dephosphorylate downstream targets and PDEs that break down cAMP and cGMP (Francis et al., 2010, 2011). The larger Ca^{2+} currents observed in the SHR neurons could be due to reduced PKG-mediated inhibition and/or increased PKA-mediated activation of the current. Because ω-conotoxin GVIA reduced the currents of both models down to similar levels, this suggests that the differences seen are due to modulation of the *N*-type Ca^{2+} channel. Moreover, we observed that currents were normalized after a 4-minute perfusion of cGMP, suggesting that changes in channel regulation rather than expression are likely to account for the differences reported here.

NO–cGMP pathway in sympathetic responsiveness

SHR sympathetic neurons have lower bioavailability of NO and reduced expression of the β_1 subunit of sGC (Li et al., 2013), resulting in lower levels of cGMP (Li et al., 2007). This is associated with increased Ca^{2+} transients (Li et al., 2012) and enhanced neurotransmission (Herring et al., 2011; Li et al., 2012; Shanks et al., 2013c) compared with control neurons. Gene transfer of nNOS (Li et al., 2013) or its adaptor protein, CAPON (Lu et al., 2015), rescues this sympathetic phenotype. However, we cannot rule out that a part of the inhibitory effect of NO modulation on $Cav_{2.2}$ is via non-GMP-mediated S-nitroylation of the channel protein itself. Zhou et al. (2015) reported in HEK 293 cells that the NO donor SNAP can generate S-nitrosothiols that block the N type conductance, an effect reversed by methanethiosulfonate ethylammonium. Moreover, they identified the consensus motifs for channel inhibition that involved several intracellular cysteine residues. In particular, site-directed mutagenesis

of cysteine 1045 in the II–III loop significantly reduced NO sensitivity of $Cav_{2.2}$. Whether this pathway is functionally activated within the range of physiological concentrations of NO remains to be established.

Nevertheless, our results provide direct evidence in sympathetic neurons that cGMP causes attenuation of the Ca^{2+} channel current. Indeed, previous studies have demonstrated that the NO–cGMP pathway can regulate Ca^{2+} currents via PKG activation, but also through cross-talk with PDEs (Méry et al., 1991; Fischmeister and Méry, 1996). Studies have reported that application of 8b-cGMP leads to a direct phosphorylation of Ca^{2+} channels via PKG (Jiang et al., 2000). This resulted in smaller currents, but no change in the voltage dependency (Tohse and Sperelakis, 1991), of the channel, which is analogous to what we describe here.

cAMP-cGMP cross-talk via PDEs

In addition to its direct effects on ion channels, cGMP can act via cross-talk with the cAMP pathway via its activation/inhibition of cellular PDEs (Zaccolo and Movsesian, 2007; Francis et al., 2010; Stangherlin et al., 2011). cGMP and cAMP compete with each other for the catalytic sites on the PDEs with varying affinities (Conti and Beavo, 2007; Francis et al., 2010), resulting in inhibition and/or activation of these enzymes. PDE2A and PDE3 have dual specificity for cAMP and cGMP (Conti and Beavo, 2007; Francis et al., 2010). cGMP activates PDE2A, leading to the breakdown of cAMP (and thus reduction in PKA-mediated phosphorylation of downstream targets including Ca^{2+} channels), whereas it can inhibit PDE3A with the opposite result. Although a cell is likely to express several PDEs that regulate the efficacy of CNs, PDE2A and PDE3A have been localized in cardiac myocytes (Stangherlin and Zaccolo, 2012a; Maass et al., 2015; Zoccarato et al., 2015), where they are critically involved in cardiac function (Stangherlin and Zaccolo, 2012a). PDE2A has been reported recently in sympathetic stellate neurons with high activity in SHR neurons (Li et al., 2015), whereas there is no direct evidence of PDE3 expression within sympathetic stellate neurons.

To test whether the cGMP dysregulation seen in the SHR was affecting cAMP signaling, we elevated cGMP levels pharmacologically and used FRET to record changes in cAMP levels. We investigated its functional relevance by assessing PKA activity. Application of 8b-cGMP led to a reduction of cAMP in SHR neurons, with no activation of PKA, suggesting that cAMP hydrolysis via cGMP stimulation of PDE2A is occurring. The cGMP-dependent reduction in the Ca^{2+} channel current after 8b-cGMP is consistent with the notion of PDE2A dominance in diseased neurons affecting the efficacy of cGMP, because overexpressing PDE2A decreases cGMP and increases intracellular Ca^{2+} transients and neurotransmission (Li et al., 2015; Seifert, 2015). Conversely, in the control neurons, even though 8b-cGMP significantly increased cAMP levels and PKA activity (suggesting the involvement of other PDEs inhibited by cGMP), this did not translate into a change in Ca^{2+} channel current because activation of the inhibitory cGMP-PKG pathway most likely counterbalanced changes in the stimulatory cAMP–PKA pathway. However, slowing cGMP hydrolysis with PDE2A inhibition markedly increased the Ca^{2+} current in normal neurons, probably as a consequence of cGMP acting to inhibit PDE3 leading to greater levels of cAMP–PKA activity (Figure 5).

Evidence of altered PDE2A/PDE3A balance in sympathetic neurons

Mutations in PDE3A have been implicated in human hypertension (Houslay, 2015; Maass et al., 2015). Given the observed increase in cAMP after administration of 8b-cGMP in control neurons, we hypothesized that PDE3 may be functionally expressed within stellate neurons, as has been demonstrated in the superior cervical ganglions (Nunes et al., 2012). The selective PDE3 inhibitor milrinone led to similar increases in cAMP levels within both SHR and control neurons. Comparable results were also observed using the clinically approved PDE3 inhibitor cilostamide. The notion of differential PDE2/3 involvement in control and diseased neurons helps to clarify the effects that PDE2A inhibition has in the regulation of the Ca^{2+} currents (Fig. 5). In control neurons, this leads to significantly increased currents, possibly due to the direct elevation of cAMP causing inhibition of cAMP hydrolysis, but also via the indirect elevation of cAMP mediated by cGMP inhibition of PDE3. This in turn may result in increased PKA-mediated phosphorylation of Ca^{2+} channel currents. Conversely, in the SHR, the net result of PDE2A inhibition is a decrease in channel currents, possibly due to cGMP-mediated channel inhibition. This is consistent with the evidence that PDE2A has a higher affinity for hydrolysis of cGMP over cAMP (Xu et al., 2013; Li et al., 2015). Altered PDE2/3 balance could therefore be linked to the dysautonomia associated with hypertension (Fig. 8).

Limitations

CNs (Mongillo et al., 2006; Stangherlin et al., 2011; Stangherlin and Zaccolo, 2012b; Lomas and Zaccolo, 2014) and PDEs reside in distinct subcellular compartments (Lefkimmiatis and Zaccolo, 2014). Specifically, in the rat, there are three splice variants of PDE2A that are localized in the cytosol (PDE2A1) or membrane (PDE2A2 and 3; Bender and Beavo, 2006), although their exact roles remain to be established. Similarly, PKA/PKG regulation of the Ca^{2+} channels also occurs in distinct signalosomes near the channels themselves, conferring site-specific regulation of Ca^{2+} entry coupled to neurotransmission (Toda and Okamura, 2003; Garthwaite, 2016). Furthermore, the rate of PDE hydrolysis is critically dependent on the concentration of both cAMP and cGMP that is reported to be different between cell types (Francis et al., 2010; Zhao et al., 2016). Although the global cAMP responses after PDE2A and PDE3 inhibition were similar between control and diseased neurons, this does not in itself establish that localized control within specifically regulated microdomains is normal in the diseased neuron.

References

Bannister RA, Meza U, Adams BA (2005) Phosphorylation-dependent regulation of voltage-gated Ca^{2+} channels. In: Voltage-gated calcium channels (G. Zamponi, ed.), pp 168–182. Boston: Springer.

Bar-Yehuda D, Korngreen A (2008) Space-clamp problems when voltage clamping neurons expressing voltage-gated conductances. J Neurophysiol 99:1127–1136. CrossRef Medline

Bender AT, Beavo JA (2006) Cyclic nucleotide phosphodiesterases: molecular regulation to clinical use. Pharmacol Rev 58:488–520. CrossRef Medline

Catterall WA (2000) Structure and regulation of voltage-gated Ca^{2+} channels. Annu Rev Cell Dev Biol 16:521–555. CrossRef Medline

Catterall WA (2011) Voltage-gated calcium channels. Cold Spring Harb Perspect Biol 3:a003947. CrossRef Medline

Conti M, Beavo J (2007) Biochemistry and physiology of cyclic nucleotide phosphodiesterases: essential components in cyclic nucleotide signaling. Annu Rev Biochem 76:481–511. CrossRef Medline

Danson EJ, Paterson DJ (2005) Cardiac neurobiology of nitric oxide synthases. Ann N Y Acad Sci 1047:183–196. CrossRef Medline

Danson EJ, Choate JK, Paterson DJ (2005) Cardiac nitric oxide: emerging role for nNOS in regulating physiological function. Pharmacol Ther 106: 57–74. CrossRef Medline

Depry C, Allen MD, Zhang J (2011) Visualization of PKA activity in plasma membrane microdomains. Mol BioSyst 7:52–58. CrossRef Medline

Dickhout JG, Lee RM (1998) Blood pressure and heart rate development in young spontaneously hypertensive rats. Am J Physiol 274:H794–H800. Medline

Esler M (2010) Sympathetic nervous activation in essential hypertension: commonly neglected as a therapeutic target, usually ignored as a drug side effect. Hypertension 55:1090–1091. CrossRef Medline

Fischmeister R, Méry PF (1996) Regulation of cardiac calcium current by cGMP/NO route. C R Seances Soc Biol Fil 190:181–206. Medline

Francis SH, Busch JL, Corbin JD, Sibley D (2010) cGMP-dependent protein kinases and cGMP phosphodiesterases in nitric oxide and cGMP action. Pharmacol Rev 62:525–563. CrossRef Medline

Francis SH, Blount MA, Corbin JD (2011) Mammalian cyclic nucleotide phosphodiesterases: molecular mechanisms and physiological functions. Physiol Rev 91:651–690. CrossRef Medline

Garthwaite J (2016) From synaptically localized to volume transmission by nitric oxide. J Physiol 594:9–18. CrossRef Medline

Grassi G, Mark A, Esler M (2015) The sympathetic nervous system alterations in human hypertension. Circ Res 116:976–990. CrossRef Medline

Heaton DA, Lei M, Li D, Golding S, Dawson TA, Mohan RM, Paterson DJ (2006) Remodeling of the cardiac pacemaker L-type calcium current and its beta-adrenergic responsiveness in hypertension after neuronal NO synthase gene transfer. Hypertension 48:443–452. CrossRef Medline

Heaton DA, Li D, Almond SC, Dawson TA, Wang L, Channon KM, Paterson DJ (2007) Gene transfer of neuronal nitric oxide synthase into intracardiac ganglia reverses vagal impairment in hypertensive rats. Hypertension 49:380–388. CrossRef Medline

Herring N, Lee CW, Sunderland N, Wright K, Paterson DJ (2011) Pravastatin normalises peripheral cardiac sympathetic hyperactivity in the spontaneously hypertensive rat. J Mol Cell Cardiol 50:99–106. CrossRef Medline

Houslay M (2015) Hypertension linked to PDE3A activation. Nat Genet 47:562–563. CrossRef Medline

Imredy JP, Yue DT (1994) Mechanism of Ca(2+)-sensitive inactivation of L-type Ca^{2+} channels. Neuron 12:1301–1318. CrossRef Medline

Ino M, Yoshinaga T, Wakamori M, Miyamoto N, Takahashi E, Sonoda J, Kagaya T, Oki T, Nagasu T, Nishizawa Y, Tanaka I, Imoto K, Aizawa S, Koch S, Schwartz A, Niidome T, Sawada K, Mori Y (2001) Functional disorders of the sympathetic nervous system in mice lacking the alpha 1B subunit (Cav 2.2) of N-type calcium channels. Proc Natl Acad Sci U S A 98:5323–5328. CrossRef Medline

Jiang LH, Gawler DJ, Hodson N, Milligan CJ, Pearson HA, Porter V, Wray D (2000) Regulation of cloned cardiac L-type calcium channels by cGMP-dependent protein kinase. J Biol Chem 275:6135–6143. CrossRef Medline

Jin XG, Chen SR, Cao XH, Li L, Pan HL (2011) Nitric oxide inhibits nociceptive transmission by differentially regulating glutamate and glycine release to spinal dorsal horn neurons. J Biol Chem 286:33190–33202. CrossRef Medline

Klarenbeek J, Goedhart J, van Batenburg A, Groenewald D, Jalink K (2015) Fourth-generation epac-based FRET sensors for cAMP feature exceptional brightness, photostability and dynamic range: characterization of dedicated sensors for FLIM, for ratiometry and with high affinity. Anderson KI, ed. PLoS One 10:e0122513. CrossRef Medline

Krukoff TL (1998) Central regulation of autonomic function: no brakes? Clin Exp Pharmacol Physiol 25:474–478. CrossRef Medline

Lefkimmiatis K, Zaccolo M (2014) cAMP signaling in subcellular compartments. Pharmacol Ther 143:295–304. CrossRef Medline

Lefkimmiatis K, Leronni D, Hofer AM (2013) The inner and outer compartments of mitochondria are sites of distinct cAMP/PKA signaling dynamics. J Cell Biol 202:453–462. CrossRef Medline

Li D, Paterson DJ (2016) Cyclic nucleotide regulation of cardiac sympathovagal responsiveness. J Physiol. In press.

Li D, Wang L, Lee CW, Dawson TA, Paterson DJ (2007) Noradrenergic cell specific gene transfer with neuronal nitric oxide synthase reduces cardiac sympathetic neurotransmission in hypertensive rats. Hypertension 50: 69–74. CrossRef Medline

Li D, Lee CW, Buckler K, Parekh A, Herring N, Paterson DJ (2012) Abnormal intracellular calcium homeostasis in sympathetic neurons from young prehypertensive rats. Hypertension 59:642–649. CrossRef Medline

Li D, Nikiforova N, Lu CJ, Wannop K, McMenamin M, Lee CW, Buckler KJ, Paterson DJ (2013) Targeted neuronal nitric oxide synthase transgene delivery into stellate neurons reverses impaired intracellular calcium transients in prehypertensive rats. Hypertension 61:202–207. CrossRef Medline

Li D, Lu CJ, Hao G, Wright H, Woodward L, Liu K, Vergari E, Surdo NC, Herring N, Zaccolo M, Paterson DJ (2015) Efficacy of B-type natriuretic peptide is coupled to phosphodiesterase 2A in cardiac sympathetic neurons. Hypertension 66:190–198. CrossRef Medline

Lomas O, Zaccolo M (2014) Phosphodiesterases maintain signaling fidelity via compartmentalization of cyclic nucleotides. Physiology 29:141–149. CrossRef Medline

Lu CJ, Hao G, Nikiforova N, Larsen HE, Liu K, Crabtree MJ, Li D, Herring N, Paterson DJ (2015) CAPON modulates neuronal calcium handling and cardiac sympathetic neurotransmission during dysautonomia in hypertension. Hypertension 65:1288–1297. CrossRef Medline

Lundin S, Ricksten SE, Thorén P (1984) Renal sympathetic activity in spontaneously hypertensive rats and normotensive controls, as studied by three different methods. Acta Physiol Scand 120:265–272. CrossRef Medline

Maass PG, Aydin A, Luft FC, Schächterle C, Weise A, Stricker S, Lindschau C, Vaegler M, Qadri F, Toka HR, Schulz H, Krawitz PM, Parkhomchuk D, Hecht J, Hollfinger I, Wefeld-Neuenfeld Y, Bartels-Klein E, Mühl A, Kann M, Schuster H, et al. (2015) PDE3A mutations cause autosomal dominant hypertension with brachydactyly. Nat Genet 47:647–653. CrossRef Medline

Mancia G, Grassi G (2014) The autonomic nervous system and hypertension. Circ Res 114:1804–1814. CrossRef Medline

McCleskey EW, Fox AP, Feldman D, Tsien RW (1986) Different types of calcium channels. J Exp Biol 124:177–190. Medline

Méry PF, Lohmann SM, Walter U, Fischmeister R (1991) Ca^{2+} current is regulated by cyclic GMP-dependent protein kinase in mammalian cardiac myocytes. Proc Natl Acad Sci U S A 88:1197–1201. CrossRef Medline

Molderings GJ, Likungu J, Göthert M (2000) N-Type calcium channels control sympathetic neurotransmission in human heart atrium. Circulation 101:403–407. CrossRef Medline

Mongillo M, Tocchetti CG, Terrin A, Lissandron V, Cheung YF, Dostmann WR, Pozzan T, Kass DA, Paolocci N, Houslay MD, Zaccolo M (2006) Compartmentalized phosphodiesterase-2 activity blunts beta-adrenergic cardiac inotropy via an NO/cGMP-dependent pathway. Circ Res 98: 226–234. CrossRef Medline

Mori Y, Nishida M, Shimizu S, Ishii M, Yoshinaga T, Ino M, Sawada K, Niidome T (2002) Ca(2+) channel alpha(1B) subunit (Ca(V) 2.2) knockout mouse reveals a predominant role of N-type channels in the sympathetic regulation of the circulatory system. Trends Cardiovasc Med 12:270–275. CrossRef Medline

Nunes AR, Sample V, Xiang YK, Monteiro EC, Gauda E, Zhang J (2012) Effect of oxygen on phosphodiesterases (PDE) 3 and 4 isoforms and PKA activity in the superior cervical ganglia. Adv Exp Med Biol 758:287–294. CrossRef Medline

Olivera BM, Cruz LJ, de Santos V, LeCheminant GW, Griffin D, Zeikus R, McIntosh JM, Galyean R, Varga J, Gray WR (1987) Neuronal calcium channel antagonists. Discrimination between calcium channel subtypes using omega-conotoxin from Conus magus venom. Biochemistry 26: 2086–2090. CrossRef Medline

Paterson D (2001) Nitric oxide and the autonomic regulation of cardiac excitability. Exp Physiol 86:1–12. CrossRef Medline

Ponsioen B, Zhao J, Riedl J, Zwartkruis F, van der Krogt G, Zaccolo M, Moolenaar WH, Bos JL, Jalink K (2004) Detecting cAMP-induced Epac activation by fluorescence resonance energy transfer: Epac as a novel cAMP indicator. EMBO Rep 5:1176–1180. CrossRef Medline

Pruneau D, Bélichard P (1992) Haemodynamic and humoral effects of omega-conotoxin GVIA in normotensive and spontaneously hypertensive rats. Eur J Pharmacol 211:329–335. CrossRef Medline

Seifert R (2015) Emerging role of phosphodiesterase 2A in hypertension. Hypertension 66:13–14. CrossRef Medline

Shanks J, Herring N (2013) Peripheral cardiac sympathetic hyperactivity in cardiovascular disease: role of neuropeptides. Am J Physiol Regul Integr Comp Physiol 305:R1411–R1420. CrossRef Medline

Shanks J, Manou-Stathopoulou S, Lu CJ, Li D, Paterson DJ, Herring N (2013a) Peripheral cardiac sympathetic dysfunction in the prehyperten-

sive spontaneously hypertensive rat. Am J Physiol Heart Circ Physiol 305:H980–H986. doi: 10.1152/ajpheart.00255.2013. CrossRef

Shanks J, Mane S, Ryan R, Paterson DJ (2013b) Ganglion-specific impairment of the norepinephrine transporter in the hypertensive rat. Hypertension 61:187–193. CrossRef Medline

Shanks J, Manou-Stathopoulou S, Lu CJ, Li D, Paterson DJ, Herring N (2013c) Cardiac sympathetic dysfunction in the prehypertensive spontaneously hypertensive rat. Am J Physiol Heart Circ Physiol 305:H980–H986. CrossRef Medline

Simms BA, Zamponi GW (2014) Neuronal voltage-gated calcium channels: structure, function, and dysfunction. Neuron 82:24–45. CrossRef Medline

Stangherlin A, Zaccolo M (2012a) cGMP-cAMP interplay in cardiac myocytes: a local affair with far-reaching consequences for heart function. Biochem Soc Trans 40:11–14. CrossRef Medline

Stangherlin A, Zaccolo M (2012b) Phosphodiesterases and subcellular compartmentalized cAMP signaling in the cardiovascular system. Am J Physiol Heart Circ Physiol 302:H379–H390. CrossRef Medline

Stangherlin A, Gesellchen F, Zoccarato A, Terrin A, Fields LA, Berrera M, Surdo NC, Craig MA, Smith G, Hamilton G, Zaccolo M (2011) cGMP signals modulate cAMP levels in a compartment-specific manner to regulate catecholamine-dependent signaling in cardiac myocytes. Circ Res 108:929–939. CrossRef Medline

Toda N, Okamura T (2003) The pharmacology of nitric oxide in the peripheral nervous system of blood vessels. Pharmacol Rev 55:271–324. CrossRef Medline

Tohse N, Sperelakis N (1991) cGMP inhibits the activity of single calcium channels in embryonic chick heart cells. Circ Res 69:325–331. CrossRef Medline

Tsuda K, Tsuda S, Nishio I, Masuyama Y (2001) Role of dihydropyridine-sensitive calcium channels in the regulation of norepinephrine release in hypertension. J Cardiovasc Pharmacol 38:S27–S31. Medline

Tu H, Liu J, Zhang D, Zheng H, Patel KP, Cornish KG, Wang WZ, Muelleman RL, Li YL (2014) Heart failure-induced changes of voltage-gated Ca^{2+} channels and cell excitability in rat cardiac postganglionic neurons. Am J Physiol Cell Physiol 306:C132–C142. CrossRef Medline

Uhrenholt TR, Nedergaard OA (2003) Calcium channels involved in noradrenaline release from sympathetic neurones in rabbit carotid artery. Pharmacol Toxicol 92:226–233. CrossRef Medline

Uhrenholt TR, Nedergaard OA (2005) Involvement of different calcium channels in the depolarization-evoked release of noradrenaline from sympathetic neurones in rabbit carotid artery. Basic Clin Pharmacol Toxicol 97:109–114. CrossRef Medline

Wang L, Henrich M, Buckler KJ, McMenamin M, Mee CJ, Sattelle DB, Paterson DJ (2007) Neuronal nitric oxide synthase gene transfer decreases $[Ca^{2+}]i$ in cardiac sympathetic neurons. J Mol Cell Cardiol 43:717–725. CrossRef Medline

Xu Y, Pan J, Chen L, Zhang C, Sun J, Li J, Nguyen L, Nair N, Zhang H, O'Donnell JM (2013) Phosphodiesterase-2 inhibitor reverses corticosterone-induced neurotoxicity and related behavioural changes via cGMP/PKG dependent pathway. Int J Neuropsychopharmacol 16:835–847. CrossRef Medline

Yamada Y, Kinoshita H, Kuwahara K, Nakagawa Y, Kuwabara Y, Minami T, Yamada C, Shibata J, Nakao K, Cho K, Arai Y, Yasuno S, Nishikimi T, Ueshima K, Kamakura S, Nishida M, Kiyonaka S, Mori Y, Kimura T, Kangawa K, et al. (2014) Inhibition of N-type Ca^{2+} channels ameliorates an imbalance in cardiac autonomic nerve activity and prevents lethal arrhythmias in mice with heart failure. Cardiovasc Res 104:183–193. CrossRef Medline

Zaccolo M, Movsesian MA (2007) cAMP and cGMP signaling cross-talk: role of phosphodiesterases and implications for cardiac pathophysiology. Circ Res 100:1569–1578. CrossRef Medline

Zamponi GW, Striessnig J, Koschak A, Dolphin AC (2015) The physiology, pathology, and pharmacology of voltage-gated calcium channels and their future therapeutic potential. Pharmacol Rev 67:821–870. CrossRef Medline

Zhao CY, Greenstein JL, Winslow RL (2016) Roles of phosphodiesterases in the regulation of the cardiac cyclic nucleotide cross-talk signaling network. J Mol Cell Cardiol 91:215–227. CrossRef Medline

Zhou MH, Bavencoffe A, Pan HL (2015) Molecular basis of regulating high voltage-activated calcium channels by S-nitrosylation. J Biol Chem 290:30616–30623. CrossRef Medline

Zoccarato A, Surdo NC, Aronsen JM, Fields LA, Mancuso L, Dodoni G, Stangherlin A, Livie C, Jiang H, Sin YY, Gesellchen F, Terrin A, Baillie GS, Nicklin SA, Graham D, Szabo-Fresnais N, Krall J, Vandeput F, Movsesian M, Furlan L, et al. (2015) Cardiac hypertrophy is inhibited by a local pool of cAMP regulated by phosphodiesterase 2. Circ Res 117:707–719. CrossRef Medline

Zugck C, Lossnitzer D, Backs J, Kristen A, Kinscherf R, Haass M (2003) Increased cardiac norepinephrine release in spontaneously hypertensive rats: role of presynaptic alpha-2A adrenoceptors. J Hypertens 21:1363–1369. CrossRef Medline